Optics Letters

Bending sensor combining multicore fiber with a mode-selective photonic lantern

Amy Van Newkirk,[1,*] J. E. Antonio-Lopez,[1] Amado Velazquez-Benitez,[1,2] Jacques Albert,[3] Rodrigo Amezcua-Correa,[1] and Axel Schülzgen[1]

[1]CREOL, the College of Optics and Photonics, the University of Central Florida, Orlando, Florida 32816, USA
[2]Instituto de Investigaciones en Materiales, UNAM, Cd Universitaria, D.F., 04510, 70-360, Mexico
[3]Department of Electronics, Carleton University, Ottawa, Ontario K1S 5B6, Canada
*Corresponding author: amy.vannewkirk@knights.ucf.edu

Received 2 September 2015; revised 29 September 2015; accepted 5 October 2015; posted 5 October 2015 (Doc. ID 249307); published 3 November 2015

A bending sensor is demonstrated using the combination of a mode-selective photonic lantern (PL) and a multicore fiber. A short section of three-core fiber with strongly coupled cores is used as the bend sensitive element. The supermodes of this fiber are highly sensitive to the refractive index profiles of the cores. Small bend-induced changes result in drastic changes of the supermodes, their excitation, and interference. The multicore fiber is spliced to a few-mode fiber and excites bend dependent amounts of each of the six linearly polarized (LP) modes guided in the few-mode fiber. A mode selective PL is then used to demultiplex the modes of the few-mode fiber. Relative power measurements at the single-mode PL output ports reveal a high sensitivity to bending curvature and differential power distributions according to bending direction, without the need for spectral measurements. High direction sensitivity is demonstrated experimentally as well as in numerical simulations. Relative power shifts of up to 80% have been measured at radii of approximately 20 cm, and good sensitivity was observed with radii as large as 10 m, making this sensing system useful for applications requiring both large and small curvature measurements.

OCIS codes: (060.2280) Fiber design and fabrication; (060.2370) Fiber optics sensors.

http://dx.doi.org/10.1364/OL.40.005188

The ability to measure the curvature of an object is extremely important in applications such as mechanical and aerospace engineering, and structural health monitoring. Additionally, knowing both the degree of curvature and the direction of the bending can be very useful in evaluating structural integrity, as these parameters can help in identifying deformations and stresses in structures. Various fiber-sensing systems have been analyzed for applications as direction-sensitive bending sensors. Most of these sensor systems employ some form of fiber grating, including long period gratings [1], cladding waveguide gratings [2], and fiber Bragg gratings in multicore fiber (MCF) [3]. Whereas these and other grating-based systems have been shown to be able to measure bending and distinguish multiple directions, writing gratings into multiple cores or the cladding of an optical fiber requires complicated fabrication techniques. Luna Technologies has developed a commercial shape sensing system based on Rayleigh scattering in MCF that has high accuracy and does not require fiber Bragg gratings. However, the optical frequency domain reflectometry method used is computationally complex and requires the sweeping of a tunable laser source, resulting in high cost instrumentation [4].

Alternatively, simpler fiber sensing systems based on MCF have been shown to work well for measuring temperature [5,6], refractive index [7], strain [8,9], as well as curvature [10–12]. These sensors utilize the coupling of the multiple cores of the MCF, which creates a modulated transmission spectrum for sensing [13]. They are generally simpler to fabricate than grating-based sensors and have comparable sensitivity. However, these MCF sensing systems generally still rely on spectral analysis instrumentation.

In this Letter we demonstrate the sensing capabilities of a MCF in conjunction with a photonic lantern (PL) [14–17], which eliminates the need for measuring the spectra of the device. PLs are all-fiber devices consisting of a number of single-mode fibers (SMF) that are fused together and tapered down to form a single multimode fiber (MMF) or few-mode fiber (FMF) [16]. Mode-selective PLs are a developing technology with applications in spatial division multiplexing for telecommunications [16,17]. In a mode-selective PL each SMF excites a different linearly polarized (LP) mode in the output FMF, with low cross-talk between the modes. Here we use the mode-selective PL to measure the power in the various modes of a FMF through the corresponding SMF outputs. The ability to decouple various modes in a fiber using an all-fiber device leads to new possibilities in the field of fiber sensing. In our experimental setup, the PL is being used in conjunction with a three-core fiber with strongly coupled cores, similar to the MCF that has already been demonstrated to be sensitive to bending [10]. This combination allows for increasing the measurement

sensitivity while relying exclusively on power measurements without the need for any form of spectral analysis.

The MCF used was fabricated in-house using the stack and draw method. The cores are 9 μm in diameter, with a pitch of 11 μm, and the fiber outer diameter is 120 μm. The fiber was fabricated from Ge-doped silica, with a Δn of 7×10^{-3} and each core had an NA of 0.14. The cross section of the MCF is shown in Fig. 1.

The mode-selective PL was also fabricated in-house by first drawing four Ge-doped graded-index fibers (GIF) with a Δn of 16×10^{-3} and core sizes of 20, 18, 15, and 6 μm. The GIFs are spliced to SMF ensuring the excitation of only the LP_{01} mode. The various core sizes will excite different LP modes in the FMF (LP_{01}, $LP_{11a,b}$, $LP_{21a,b}$, and LP_{02}, respectively) [17]. Six GIFs are then inserted into a low index capillary made of fluorine-doped glass with a Δn of -9×10^{-3} relative to fused silica in the arrangement shown in Fig. 1. The filled capillary is then tapered using a CO_2 laser tapering station (LZM-100 by AFL). As the device is tapered with a final taper ratio of 15.9:1 over 50 mm length, the individual cores become negligible and the light is guided in the cladding of the GIFs that, in the tapered section, form a FMF with a core size of 18 μm. This end of the lantern is spliced to a FMF with a core size of 15 μm and a Δn of 11×10^{-3} that supports only the six LP modes previously mentioned.

The experimental setup used is shown in Fig. 1. A superluminescent diode (SLD) centered at 1550 nm is used as the light source, and a SMF is used to excite the various supermodes in the MCF with three strongly coupled cores, with one of the three cores being centrally aligned with the core of the SMF. This fiber supports three polarization degenerate supermodes, as shown in Fig. 2(b). There will be supermode interference within the MCF [13]; however, by using a very short section of MCF, the spectral period of the interference pattern will be hundreds of nanometers, and the interference fringes will be outside of the SLD bandwidth. For this test we used 0.5 cm of a three-core fiber that had a smooth transmission spectrum throughout the ~40 nm bandwidth of the SLD.

The MCF is then spliced to the FMF end of the PL that supports the six LP modes shown in Fig. 2(c). The power through the SMF outputs of the lantern is then measured with an integrating sphere (IS).

The MCF section is bent with a controlled direction and radius of curvature by fixing the fiber inside of a plastic tube and forcing it to bend through the inward movement of a translation stage in a similar setup to [10]. Bending the MCF changes the refractive index profile, and therefore

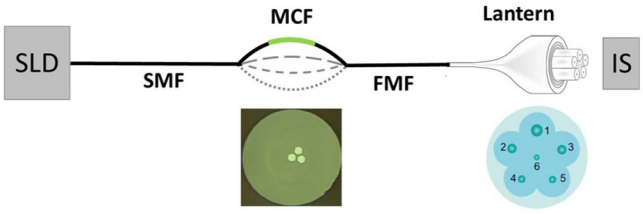

Fig. 1. Schematic of the experimental setup, including cross section of the three-core fiber used, and a schematic of the arrangement of graded index fibers within the PL (1, 20 μm; 2 and 3, 18 μm; 4 and 5, 15 μm; 6, 6 μm core diameter).

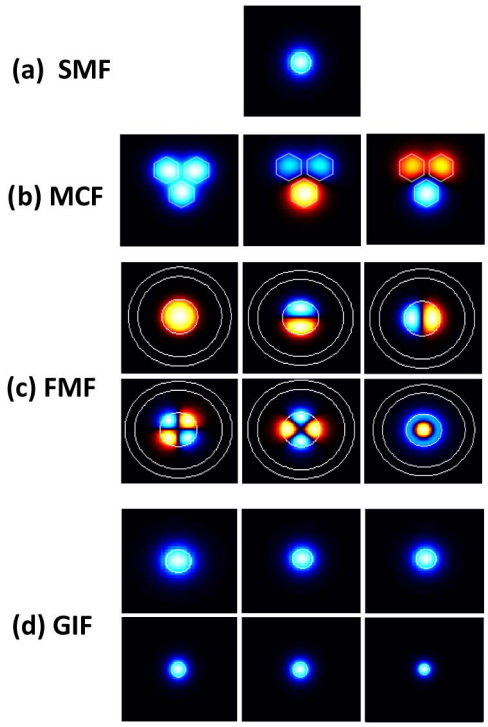

Fig. 2. Simulated mode profiles of the fiber modes from each section of the fiber bending sensor device: (a) standard SMF, (b) three-core fiber, (c) FMF, and (d) the fundamental modes of the GIFs with varying core diameters at the output of the PL.

changes the supermodes, their excitation from the SMF, and their propagation. This in turn changes the FMF modes that are excited by the MCF and their relative powers. The power in each of the FMF modes can be measured with the SMF outputs of the PL. The change in relative power of each mode is then measured as a function of radius and direction of the MCF bending.

Before discussing the relative power measurements, it needs to be verified that, in fact, a change of the excited power of the FMF modes is observed and not a spectral shift due to multimode interference. To do so, the transmission spectra were recorded as the MCF was bent. As shown in Fig. 3, the total power of mode LP_{11a} transmitted through the PL does in fact increase and decrease with bending, with no noticeable spectral shift. Figure 3(a) shows the interference fringes caused by the multiple excited modes of the FMF. However, they do not shift as the MCF is bent in either direction by a radius of 23 cm. Figure 3(b) shows smoothed spectra that clearly show the total change in power for this mode, which for the same bending radius is clearly dependent on the bending direction.

The relative power shift (change in power/initial power or $\Delta P/P_o$) measured for each of the six lantern modes for four bending directions is shown in Fig. 4. Clearly, each mode power responds differently to bending, and this response is direction sensitive. The relative power change measured was as high as 80% for some modes, providing exceptional sensitivity. It was observed that the change in relative power is sometimes linear with respect to the inverse radius of curvature, and is sometimes curved, depending on the mode and the direction of bending. The highest sensitivity observed experimentally was

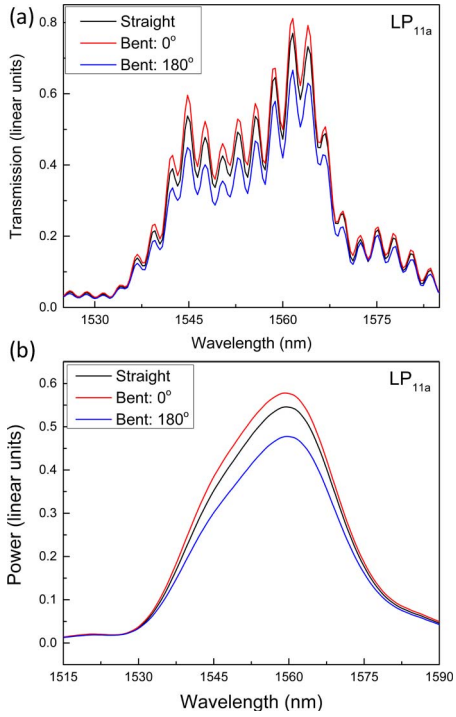

Fig. 3. Transmission spectra of the LP_{11a} mode when bent in two directions with a radius of 23 cm, with spectral smoothing applied during the post processing. (a) A nine-point Savitzky–Golay smoothing filter was used showing the multimode interference occurring within the FMF, and (b) with a 65-point filter, more clearly showing the total power difference.

in the direction of 270° for the LP_{21a} mode, with 20.2%/m^{-1} with respect to the inverse radius over the region from 0.01 to 0.04 cm^{-1}, or 2.3%/cm with respect to the radius of curvature from 20 to 40 cm.

In the future, the variations in sensitivity with bending direction could be more easily understood if the experiments were designed in such a way that enabled knowledge of the MCF orientation within the bending setup. However, we currently do not have that knowledge. With six modes, each having different responses to bending, enough information can be obtained in order to fully measure the angle and the radius of curvature of the bend simultaneously.

In order to verify the necessity of the MCF as the bend-sensitive element, the experiment was repeated with the previous setup, but with a section of the FMF being bent while the MCF was kept straight. Bending the FMF resulted in very small changes in the power of the modes. The total relative power shift was less than 4% for all modes and bending directions, with the average being only 1.6% at a radius of 27 cm. The sensitivity is clearly significantly lower than that measured while bending the MCF section, showing that the high sensitivity of this system is dependent on the strong coupling of the supermodes in the MCF.

To gain predictive capabilities in designing an optimized 3D fiber optic bending sensor, the device performance was simulated using commercial waveguide software FIMMWAVE, by Photon Design. The SMF–MCF–FMF fiber chain was created in the software, and bending was applied to the MCF segment with full control over both the radius of curvature and the direction of the bend. The power in each of the FMF modes was then calculated as a function of inverse bend radius for several

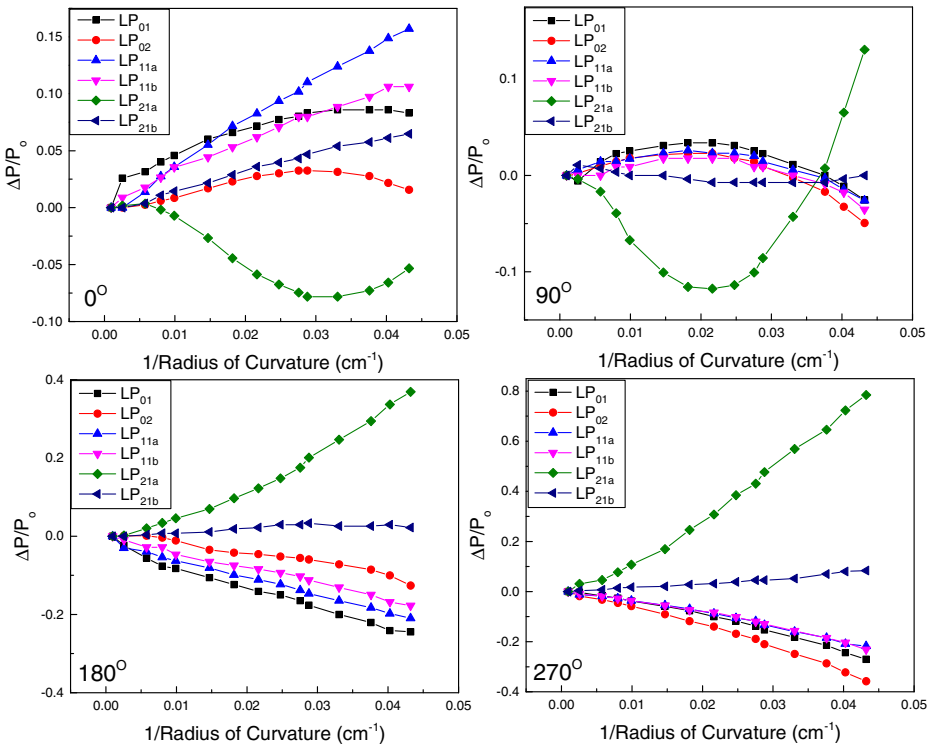

Fig. 4. Relative power shifts of each of the FMF modes measured as a function of the inverse radius of curvature for four different bending directions.

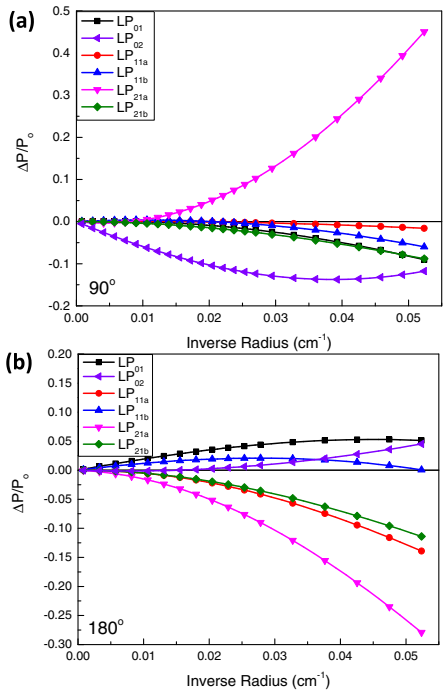

Fig. 5. Simulated relative power shifts of each mode as a function of inverse radius for two bending directions, (a) 90° and (b) 180°.

different bending directions. Figure 5 shows very similar slopes and total relative power changes to those measured experimentally, giving confidence to the accuracy of the sensing system. In addition, the simulations show a large directional dependency. Figure 5(a) was calculated for a bending direction of 90° and Fig. 5(b) was calculated for 180°. Because the orientation of the three MCF cores is not known experimentally, an exact match between the measured mode power shifts and those in simulation could not be obtained.

In addition, the combined MCF and PL device can be multiplexed for multiple point measurements by connecting the LP_{01} SMF of one device to the next input SMF in a chain, enabling the reconstruction of the full 3D shape of the fiber using the remaining five modes of each device. A similar mutliplexing technique was recently used with fiber Bragg gratings in cladding waveguides of a fiber [2]. However, this method requires a spectrometer, whereas the MCF with PL approach requires only a powermeter as the interrogation system, and has orders of magnitude higher sensitivity than the grating approach.

In conclusion, we have shown a direction-sensitive bending sensor, utilizing the combination of a MCF with a mode-selective PL. This is the first time, to our knowledge, that a PL has been used for shape sensing applications. Our results show high sensitivity to bending over a wide range of radii of curvature, as large as 10 m, making this approach useful for applications requiring knowledge of the curvature and direction of bending for small curvature applications.

REFERENCES

1. P. Saffari, T. Allsop, A. Adebayo, D. Webb, R. Haynes, and M. M. Roth, Opt. Lett. **39**, 3508 (2014).
2. C. Waltermann, A. Doering, M. Köhring, M. Angelmahr, and W. Schade, Opt. Lett. **40**, 3109 (2015).
3. D. Barrera, I. Gasulla, and S. Sales, J. Lightwave Technol. **33**, 2445 (2015).
4. R. G. Duncan, M. E. Froggatt, S. T. Kreger, R. J. Seeley, D. K. Gifford, A. K. Sang, and M. S. Wolfe, Proc. SPIE **6530**, 65301S (2007).
5. J. E. Antonio-Lopez, Z. S. Eznaveh, P. LiKamWa, A. Schülzgen, and R. Amezcua-Correa, Opt. Lett. **39**, 4309 (2014).
6. Z. Zhao, M. Tang, S. Fu, S. Liu, H. Wei, Y. Cheng, W. Tong, P. P. Shum, and D. Liu, Appl. Phys. B **112**, 491 (2013).
7. Z. Li, C. Liao, Y. Wang, X. Dong, S. Liu, K. Yang, Q. Wang, and J. Zhou, Opt. Lett. **39**, 4982 (2014).
8. A. Van Newkirk, J. E. Antonio-Lopez, G. Salceda-Delgado, M. U. Piracha, R. Amezcua-Correa, and A. Schülzgen, IEEE Photon. Technol. Lett. **27**, 1523 (2015).
9. R. M. Silva, M. S. Ferreira, J. Kobelke, K. Schuster, and O. Frazão, Opt. Lett. **36**, 3939 (2011).
10. G. Salceda-Delgado, A. Van Newkirk, J. E. Antonio-Lopez, A. Martinez-Rios, A. Schülzgen, and R. A. Correa, Opt. Lett. **40**, 1468 (2015).
11. Z. Ou, Y. Yu, P. Yan, J. Wang, Q. Huang, X. Chen, C. Du, and H. Wei, Opt. Express **21**, 23812 (2013).
12. J. R. Guzman-Sepulveda and D. A. May-Arrioja, Opt. Express **21**, 11853 (2013).
13. A. Van Newkirk, E. Antonio-Lopez, G. Salceda-Delgado, R. Amezcua-Correa, and A. Schülzgen, Opt. Lett. **39**, 4812 (2014).
14. S. G. Leon-Saval, T. A. Birks, J. Bland-Hawthorn, and M. Englund, Opt. Lett. **30**, 2545 (2005).
15. N. K. Fontaine, R. Ryf, J. Bland-Hawthorn, and S. G. Leon-Saval, Opt. Express **20**, 27123 (2012).
16. T. A. Birks, I. Gris-Sánchez, S. Yerolatsitis, S. G. Leon-Saval, and R. R. Thomson, Adv. Opt. Photon. **7**, 107 (2015).
17. A. M. Velazquez-Benitez, J. C. Alvarado, G. Lopez-Galmiche, J. E. Antonio-Lopez, J. Hernández-Cordero, J. Sanchez-Mondragon, P. Sillard, C. M. Okonkwo, and R. Amezcua-Correa, Opt. Lett. **40**, 1663 (2015).